

https://dspace.org/

Performance enhancement of flatplate and parabolic trough solar collection using nanofluid for water heating application

M AbdEl-Rady; Yasser Elhenawy; M Bassyouni; Thokozani Majozi; M Toderas ...

https://hdl.handle.net/10539/40506
SCOPUS

Downloaded from a DSpace repository. https://dspace.org/

Results in Engineering 21 (2024) 101673

Contents lists available at ScienceDirect

Results in Engineering

journal homepage: www.sciencedirect.com/journal/results-in-engineering

Performance enhancement of flat-plate and parabolic trough solar collector using nanofluid for water heating application

Mostafa AbdEl-Rady Abu-Zeid [a], Yasser Elhenawy [b,c], Mohamed Bassyouni [d,e,f,*], Thokozani Majozi [c], Monica Toderas [g,**], O.A. Al-Qabandi [h], Sameh Said Kishk [a]

[a] Department of Agricultural Engineering, Faculty of Agriculture, Suez Canal University, Ismailia 41522, Egypt
[b] Department of Mechanical Power Engineering, Faculty of Engineering, Port Said University, 42526, Egypt
[c] School of Chemical and Metallurgical Engineering, University of the Witwatersrand, 1 Jan Smuts Avenue, Johannesburg, 2000, South Africa
[d] Department of Chemical Engineering, Faculty of Engineering, Port Said University, 42526, Egypt
[e] Center of Excellence in Membrane-Based Water Desalination Technology for Testing and Characterization (CEMTC), Port Said University, Port Said, 42526, Egypt
[f] East Port Said University of Technology, North Sinai 45632, Egypt
[g] Oradea, Faculty of Sciences, University St. No.1. Oradea, 410087, Romania
[h] College of Engineering and Technology, American University of the Middle East, Egaila 54200, Kuwait

ARTICLE INFO

Keywords:
Solar collector
Nanofluid
Thermal efficiency
Greenhouse gas

ABSTRACT

Flat plate solar collector (FPSC) and parabolic trough solar collector (PTSC) are widely used for residential solar water heating (SWH) applications. This work studied two different solar collector systems. Nanofluid and its influence on the residential solar water heating (SWH) systems were investigated. The two SWH systems were designed, installed, tested, and compared at varying mass flow rates (m_f) of 0.47, 1.05, and 1.75 kg min^{-1} in ambient environmental conditions. The comparative study was conducted according to thermal efficiency (η_{th}), useful energy gain (Q_U), stored energy (Q_S), outlet hot water temperature (T_o), and difference temperature (ΔT) between the cold inlet and hot outlet water from the collectors. The analysis of outcomes showed that the PTSC was more efficient than FPSC. The FPSC and PTSC systems performance were investigated using two different types of nanofluids. Carbon nanotubes in water and ethylene glycol were utilized. A remarkable improvement in the average thermal efficiency 64.1 % and 80.6 % of FPSC and PTSC systems using ethylene glycol nanofluid were obtained respectively. The total reduction in CO_2 emissions was 31.26 kg/day and 39.28 kg/day for the FPSCs and PTSCs, respectively in the presence of ethylene glycol nanofluid. A significant saving in CO_2 release is owing to the renewable clean energy of solar collectors.

1. Introduction

Energy is necessary in our daily life. In many countries, energy consumption is rising on a daily basis, and the gap between supply and demand is continuously increasing over time as a result of people seeking a better way of life, overpopulation, and rapid industrialization [1]. Moreover, the inefficient usage of energy (*i.e.,* fossil fuels) leads to pollution of the environment. To avoid a global disaster, humanity has prioritized the use of renewable energy as a key energy source in their energy plans [2]. Solar energy is the most widely used since it is continuous, environmentally friendly, and has a low operating cost [3]. Solar energy is one of the most promising renewable energy sources for achieving sustainability and reducing the negative effects of global warming [4]. Solar thermal collectors play a vital role in utilizing solar energy for heating purposes [5]. They absorb solar radiation and convert it into thermal energy, which can be utilized for heating water [6]. Flat-plate solar collectors (FPSC) consist of a flat absorber plate that is typically made of metal, such as copper or aluminum, with a dark coating to enhance sunlight absorption. The plate is covered with a transparent glass or plastic cover to minimize heat loss. Flat-plate solar collectors (FPSCs) are widely used due to their simplicity, cost-effectiveness, and reliability [7]. Evacuated tube solar collectors (ETSCs) consist of multiple glass tubes, each containing an absorber tube. The absorber tube is surrounded by a vacuum, which minimizes

* Corresponding author. Department of Chemical Engineering, Faculty of Engineering, Port Said University, 42526, Egypt.
** Corresponding author.
E-mail addresses: m.bassyouni@eng.psu.edu.eg (M. Bassyouni), monicatoderas@gmail.com (M. Toderas).

https://doi.org/10.1016/j.rineng.2023.101673
Received 20 October 2023; Received in revised form 6 December 2023; Accepted 9 December 2023
Available online 14 December 2023
2590-1230/© 2023 The Authors. Published by Elsevier B.V. This is an open access article under the CC BY-NC-ND license (http://creativecommons.org/licenses/by-nc-nd/4.0/).

heat loss through conduction and convection. The absorber tubes are usually made of metal with a selective coating to maximize solar absorption. Evacuated tube solar collectors are known for their high efficiency, especially in colder climates or areas with low solar radiation. Parabolic Trough Collectors (PTSCs) use curved mirrors in the shape of parabolic troughs to focus sunlight onto a receiver tube placed along the focal line [7]. The receiver tube contains a heat transfer fluid (such as oil or water) that absorbs the concentrated solar energy and transfers it to heat. They are often used in large-scale solar thermal power plants but can also be utilized for water heating applications. Each type has its own unique advantages and disadvantages, and the selection of a particular type depends on various factors such as climate, location, and system requirements [8,9]. High convective and conductive heat loss has a significant impact on FPSC performance and limits its usage at high working fluid temperatures [10,11].

Several studies have investigated the thermal performance of flat-plate solar collectors (FPSCs) utilized for a variety of applications. According to Bhowmik and Amin [12], a comparative study was conducted for both standard and modified FPSCs (equipped with a reflective surface). The findings showed that the modified FPSCs exceeded the standard FPSCs notably in terms of achieving the highest thermal efficiency (η_{th}) up to 51 % maximum value. The comparative experimental investigation conducted by Said et al. [13] studied the use of a heat transfer nanofluid (FPSC) containing 0.3 % volume concentration of titanium dioxide (TiO_2) in water. The study aimed to evaluate the impact of this nanofluid on thermal efficiency under climatic conditions in Kuala Lumpur, Malaysia. According to the findings of this study, the thermal efficiency was improved to 76.6 % in the presence of FPSC nanofluid. In contrast, the thermal efficiency was reported to be 42.1 % without using nanofluid. These results suggest that the addition of 0.3 % vol TiO_2 as a heat transfer nanofluid significantly enhanced the thermal efficiency compared to the absence of nanoparticles. It indicates that the nanofluid enhanced heat transfer properties, leading to higher thermal efficiency. It was observed that the η_{th} was affected greatly by changing the spacing of collector tube [14]. In other study, a solar thermal collector running with a forced circulation pump and utilizing of aluminum nanofluid was designed by Mongre & Gupta [15]. It was reported that increasing the glazing area enhanced remarkably the η_{th} of SWH system up to 55.24 %. Likewise, the SWH system performance integrated with FPSC was tested by Ayompe & Duffy [16]. It was noticed that the average thermal efficiency was 45.6 % under the modest climate conditions of Dublin, Ireland.

Colloids or suspensions of nanoparticles in conventional liquids are known as nanofluids [17,18]. Numerous types of nanomaterial (metals, metal oxides, polymers, and carbon compounds) find use in the preparation of nanofluids for various applications. For nanofluid applications, copper, alumina, titania and copper oxide have been used most frequently. These substances are incorporated into different fluids with the primary aim of improving the ultimate physical characteristics of the mixture. The range of technological applications for this practice is extensive and continues to grow. The practice of augmenting fluids with solid particles to alter their properties has been recognized [19]. These nanoparticles can be found in a variety of liquids, such as water, ethylene glycol, kerosene, oils, refrigerants, ionic fluids, and others. Thermal stability, heat capacity, viscosity, freezing, and boiling points are taken into account while choosing base liquid [20,21]. The base liquid should not react with nanoparticles or cause their deterioration. It also should be safe, non-corrosive, and has low viscosity with no agglomeration form to prevent pumping cost increase. Nanofluids have found remarkable uses in heat transfer, bubbling heat transfer, as well as evaporation and condensation [22–24]. Brownian movement, thermophoresis, fluid layering, clustering, and ballistic transport are among the several mechanisms that contribute to the enhancement of nanofluid thermal characteristics [25–29]. They are held upright by the numerous gravitational and attraction forces operating on the liquid's nanoparticles. According to research [30–34], nanofluids can enhance the heat transfer coefficient in both natural and forced convection when compared to traditional liquids. The fundamental reason for this is the high heat conductivity of nanofluids owing to the loading of nanoparticles.

Recently, the impact of two different types of absorber materials on the PTSC performance was studied for hot water supply. Copper and aluminum nanofluid were tested at five different flowrates m_f [26]. It was noticed that the nanofluid using copper nanoparticles achieved thermal efficiency η_{th} up to 74.5 % which was higher than aluminum nanofluid (72.7 %). In another study, the optimization of a small scale PTSC (1.5 m^2) was executed by Faheem et al. [27] using Matlab simulation program. In this investigation, the η_{th} and thermal performance of PTSC were examined at two various East-West and North-South orientations.

It was stated that PTSCs exhibit better thermal efficiency (η_{th}) and performance when oriented in the East-West direction (61.66 %) compared to the North-South direction (48.28 %) [28]. This variation in performance can be attributed to factors such as solar heat flux, collector area, absorber tube arrangement, overall heat loss coefficient, and mass flow rate (m_f) [29,30]. Hot water was produced at average temperature 50 $^{\circ}$C per day with an average η_{th} of 49 % which was considerable higher than that of the FPSC [31]. The use of nanofluids in solar collectors was investigated as a means to enhance their performance compared to conventional water-based systems [35]. Studies showed that utilizing nanofluids as the working medium in solar collectors improved heat transfer characteristics and overall system performance [36]. The presence of nanoparticles in the fluid enhances thermal conductivity, which facilitates heat absorption from the solar collector's absorber surface. This, in turn, can increase the thermal efficiency of the system [37]. Carbon nanotubes (CNTs) have been specifically studied as an efficient nanomaterial for use in parabolic trough collectors (PTSCs) [38]. Carbon nanotubes have excellent thermal conductivity and unique structural properties, making them suitable candidates for enhancing heat transfer in solar thermal systems [39]. When used as a working medium in PTSCs, CNT-based nanofluids showed potential in improving the overall performance and efficiency of the collectors [40]. However, it is important to note that the use of nanofluids in practical applications requires further research and development [41]. Challenges such as nanoparticle stability, cost-effectiveness, and long-term reliability need to be addressed before widespread implementation can be realized [42]. Nevertheless, the investigation of nanofluids, including carbon nanotube-based fluids, holds promise for enhancing the performance of solar collectors and advancing solar thermal technologies. Based on the findings of the PTSC research, it has been determined that nanofluid has a significant potential to enhance the effectiveness of the solar collector [43–46]. It was reported that the performance of the solar collector would be worked on much better in the presence of nanofluid rather than water, which are tied to the thermo-physical and chemical features of liquids [47]. Carbon nanotubes were also found to be a suitable working medium for PTSC devices [48]. These issues fostered the use of solar energy in numerous solar thermal applications, including hot water delivery, space cooling, and heating. These applications are provided with various types of solar collectors, depending on the desired outlet hot water temperature (T_o) and thermal collector efficiency (η_{th}). The performance enhancement of the residential SWH system associated mainly with η_{th}. As a result, the present study was focused on the most common solar thermal collector types, FPSC and PTSC, at variable flow rates (m_f) using two different types of nanofluid and investigated the preferable system in terms of thermal efficiency (η_{th}).

2. Materials and methods

Comparative study on the FPSC and PTSC in the presence of nanofluid for residential SWH systems was performed in latitude 30.62° N, longitude 32.27° E at 5 *m* above sea level.

2.1. Experimental set-up

The flow diagrams of the two investigated SWH systems are illustrated schematically in Fig. 1(a) and (b). The designed SWH systems consist of FPSC and PTSC, hot water storage tanks and circulation pumps. A hot water storage tank was made of a plastic material with 120-L capacity and 2 mm thickness. A storage hot water tank and connected hosepipes (20 mm diameter) were used to supply water to the solar collector. The storage hot water was insulated by using a glass wool insulator (50 mm thickness and 0.03 W/(m.K) thermal conductivity) to avoid heat loss into the environment. The flat plate solar collector (FPSC) and PTSC were designed to heat up a thermal carrier water circulating into the collector tubes by absorbing solar radiation and transferring heat into water. In the parabolic trough solar collector (PTSC), solar radiation contained receiver tube where water continually circulated in a closed cycle. The collectors were attached closely together and have forced circulation utilizing a 375 Watt circulation pump. The flat plate solar collector was placed in the south direction with a slope of 31° to maximize the solar intensity and to transfer the maximum possible solar radiation.

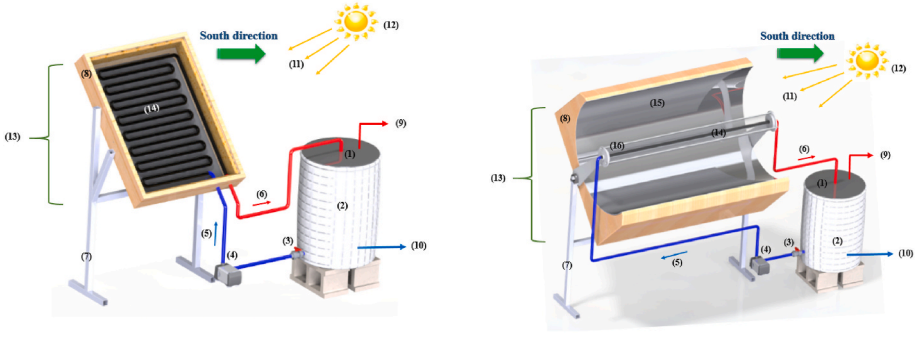
The designed rectangular shape water heating FPSC consists of an absorber plate, copper pipes, transparent glass cover, panel box, and insulation material. To absorb solar energy radiation, the top surface of the matt black paint absorber of solar collector was covered with 3 mm thick transparent glass. A transparent glass cover was sealed with a silicon rubber material for more tightness. A wooden box with a surface area of 1.44 m^2 and dimensions of 1.60 *m* length, 0.90 *m* width, and 0.10 *m* depth was fabricated to enclose the other collector components. To maximize the absorption of solar radiation, the plate and pipe were coated with a matt black paint. This type of paint was selected because it has high absorptivity as it can absorb a significant amount of solar radiation. By maximizing the absorptivity, more solar energy can be absorbed and converted into heat. The absorbing plate, made of aluminum, was used due to its high thermal conductivity, allowing it to efficiently transfer the absorbed heat to the fluid flowing through the collector. The plate has a thickness of 1 mm, which is relatively thin and helps facilitate heat transfer. Inside the absorber, serpentine copper tubes (26 *m* tube length, 8 mm diameter, 30 channels with 50 mm pitch between tubes) were fixed to pass the thermal carrier water. The pipe was arranged in a zig-zag pattern, which helped increase the contact area between the fluid and the absorbing plate. This arrangement allows for better heat transfer from the plate to the water flowing through the pipe. An insulation material of Styrofoam (0.05 *m* thick and 0.04 W $m^{-1}K^{-1}$ thermal conductivity) was fixed at the bottom of the collector to minimize the conductive heat loss through the absorber plate. The fabricated PTSC consists of cylindrical reflector, support structure and receiver tube. The PTSC is not covered with glass. Receiver consists of absorber tube positioned in the focal line of the cylindrical parabolic trough. Absorber tube made of copper material coated with a matt black paint. The solar absorptivity of the matt black paint is 99 % in order to absorb as much solar radiation. When fluid passes through the collector, it absorbs the heat generated by the absorption of solar energy. Thus, hot fluid can then be stored in a tank or used directly for hot water applications. Stainless steel AISI-304 was selected for constructing the support structure for solar collectors because it provides excellent mechanical strength and durability, as well as being readily available and relatively low cost. Stainless steel is a commonly used material for constructing the cylindrical reflector in parabolic trough collectors. Stainless steel offers several advantages over other materials such as high reflectivity, durability, and resistance to corrosion and degradation from exposure to harsh environmental circumstances. Materials selection for solar collector components is an important factor in determining the overall efficiency, durability, and lifespan of the system. Factors such as cost, availability, performance, and environmental considerations should be taken into account when selecting materials for solar collector components. AISI-304 with 0.4 mm thick, a half-accepted angle of 36.5o and concentration ratio (C) of 1.69. Properties of the stainless steel AISI-304 reflector are listed in Table 1 [49,50] and the dimensions of cylindrical PTSC are found in Table 2.

2.2. The experimental proceedings and measurements

The experiment was carried out from 8:00 a.m. to 4:00 p.m. in the ambient environmental conditions in July. The glass cover, stainless steel AISI-304 reflector, and receiver tube were cleaned out carefully before use. Measurements were recorded every 5 min and the average value was considered every hour. The meteorological station (Vantage Pro 2, Davis) was utilized to determine solar radiation intensity (I) incident on a horizontal surface (pyranometer), dry-bulb and wet-bulb temperatures, air temperature (T_a), and wind speed (W). The temperature values were permanently monitored by twelve calibrated positions at the inlet (T_i) and outlet (T_o) of the solar collectors and inside the hot

Table 1
Properties of the used stainless steel reflecting mirror.

Properties	Values
Melting point	1670 K
Density, ρ	7901 kg/m^3
Specific heat, Cp	478 J/KgK
Thermal conductivity, K	14.90 W/mk
Thermal diffusivity, θ	3.958106 m^2/s



(a) FPSC **(b) PTSC**

Fig. 1. The flow diagrams of the (a) FPSC and (b) PTSC used in the investigation: (1) Insulated hot water storage tank, (2) Glass wool insulator, (3) Faucet, (4) Circulation pump, (5) Cold feed solution, (6) Hot feed solution, (7) Iron stand, (8) Wooden box, (9) Residential hot water, (10) Residential cold water, (11) Solar radiation, (12) Sun, (13) Solar collector, (14) Absorber black copper tube, (15) Reflector, (16) Transparent receiver tube.

Table 2
Specification of cylindrical parabolic trough solar collector (PTSC).

Items	Values
Collector length	1.50 *m*
Collector width	1.0 *m*
Collector depth	0.46 *m*
Collector area	1.5 m^2
Internal diameter of absorber	0.006 *m*
Outside diameter of absorber	0.008 *m*
Inside diameter of transparent tubular receiver	0.120 *m*
Outside diameter of transparent tubular receiver	0.123 *m*
Transparent tubular receiver length	1.510 *m*

water storage tanks (T_s).

2.3. Materials and procedures

All of the tests have used chemical additives of reagent-grade. Nanofluid of Multi-walled carbon nanotubes (MWCNTs) with a 99.99 % purity and a 50 nm diameter (Sigma-Aldrich GmbH) were used. Multi-walled carbon nanotubes were selected to be used to enhance the thermal properties of fluids in the solar thermal collectors. MWCNTs-based nanofluids have higher thermal conductivity compared to traditional fluids, which helps improve the overall efficiency of the solar thermal system. In addition to their high thermal conductivity, MWCNTs-based nanofluids also have a low density and low settling rate (due to the prevalence of Brownian movement), which makes them more stable and less likely to settle or clog the system. This stability is important for maintaining the optimal performance of the solar thermal system over time [51]. The useful thermal energy extracted during the heating phase of a nanofluid containing MWCNTs can be calculated based on several key characteristics, including (i) Density (ρ_{nf}): The density of a nanofluid is important because it affects its thermal properties. Generally, as the concentration of MWCNTs in the nanofluid increases, the density of the nanofluid also increases. The density of the nanofluid can be measured using techniques such as pycnometry or densitometry [52], (ii) Heat capacity (C_{nf}): The heat capacity of a nanofluid is a measure of its ability to store heat energy. It is affected by both the base fluid and the MWCNTs. Generally, as the concentration of MWCNTs in the nanofluid increases, the heat capacity of the nanofluid also increases. The heat capacity of the nanofluid can be measured using techniques such as calorimetry. (iii) MWCNTs loading: The loading of MWCNTs in the nanofluid is an important parameter that affects the thermal properties of the nanofluid. As the loading of MWCNTs increases, the thermal conductivity of the nanofluid also increases [53]. However, there is an optimal loading of MWCNTs beyond which the thermal conductivity may decrease due to aggregation or sedimentation of the nanoparticles [54]. The loading of MWCNTs in the nanofluid can be varied and optimized to achieve the desired thermal properties.

The density and heat capacity of nanofluids at various MWCNTs loadings were estimated by eqs. (1) and (2) [55].

$$\boldsymbol{\rho}_{nf} = (1 - \varphi)\boldsymbol{\rho}_{bf} + \varphi\boldsymbol{\rho}_{s} \tag{1}$$

$$(\boldsymbol{\rho}\cdot C)_{nf} = (1 - \varphi)(\boldsymbol{\rho}\cdot C_s)_{bf} + \varphi(\boldsymbol{\rho}_s\cdot C_s)_{p} \tag{2}$$

where fluid, nanoparticles, and nanofluid are designated by the subscriptions f, p, and nf. Volume fraction is (φ).

In the thermal conductivity of a nanofluid, several factors play a crucial role. These factors include: (i) Volume Fraction (*&varphi*) of nanoparticles, as the volume fraction increases, the thermal conductivity of the nanofluid generally tends to increase as well, assuming all other factors remain constant, (ii) Thermal conductivity of the base fluid (Kf), a higher thermal conductivity of the base fluid leads to higher thermal conductivity of the nanofluid, (iii) Thermal conductivity of nanoparticles (Ks), high thermal conductivity of nanoparticles can significantly enhance the overall thermal conductivity of the nanofluid, (iv) Shape Factor, It takes into consideration factors like aspect ratio, size, and shape irregularities and nanoparticles with more elongated shapes (e.g., nanotubes) may have different thermal conductivities compared to spherical nanoparticles,(v) Interfacial thermal resistance, the interfacial thermal resistance refers to the resistance to heat transfer at the interface between the nanoparticles and the base fluid. Lower interfacial thermal resistance leads to better heat transfer between the nanoparticles and the fluid, (vi) Brownian motion, it is the random motion of particles suspended in a fluid medium due to their collisions with fast atoms or molecules. It can enhance thermal conductivity by increasing the effective contact between nanoparticles, (vii) Thermophoresis, it is the motion of particles in a fluid medium due to temperature gradients. It can affect the distribution of nanoparticles in the fluid accordingly, impact the overall thermal conductivity, (vii) agglomeration and dispersion, the state of dispersion of nanoparticles in the base fluid is crucial. Agglomeration reduces the effective surface area available for heat transfer, and (ix) Temperature, The temperature of the nanofluid affects the thermal conductivity. Some nanofluids may exhibit different thermal conductivities at different temperatures. The models used to predict the thermal conductivity of nanofluid are listed in Table 3.

The thermal conductivity of MWCNTs nanofluid generally increases with higher concentrations of MWCNTs. Additionally, the type of base fluid used can also impact the thermal conductivity of the nanofluid. Thermal conductivity of MWCNTs, water and ethylene glycol are listed in Table 4.

Table 3
Used models to predict the thermal conductivity of nanofluid.

Thermal conductivity	Parameters	Ref.
$\frac{K_{eff}}{K_f} = \frac{K_s+2K_f+2(K_s-K_f)(1+\beta)^3\varnothing}{K_s+2K_f-\varnothing(K_s-K_f)(1+\beta)^3\varnothing}$	Keff: Thermal conductivity of the nanofluid Kf: Thermal conductivity of the base fluid. Ks: Thermal conductivity of the nanoparticles φ is the particle volume fraction β:=h/r is the ratio of the nanolayer thickness (h) to the original particle radius (r).	[56]
$\frac{K_{eff}}{K_f} = \frac{K_s+2K_f+2\varnothing(K_s-K_f)}{K_s+2K_f-\varnothing(K_s-K_f)}$		[57]
$\frac{K_{eff}}{K_f} = \frac{K_s+(n-1)K_f-(n-1)(K_f-K_s)\varphi}{K_s+(n-1)K_f+(K_f-K_s)\varphi}$	n: Empirical shape factor 3/ψ ψ: The sphericity (sphericity is 1 and 0.5 for the spherical and cylindrical shapes)	[56]
$K_{eff} = K_{static} + K_{Brownian}$ $= K_p[1+\frac{3\left(\frac{K_s}{k_f}-1\right)\varnothing}{\left(\frac{K_s}{k_f}+2\right)-\left(\frac{K_s}{k_f}-1\right)\varnothing}] + 5\times10^4\gamma$ $\varphi\rho_f C_P\left[\frac{K_s T}{d_s\rho_s+2K_f-\varnothing(K_f-K_s)}\right]$	kstatic: Thermal conductivity enhancement due to the higher thermal conductivity of the nanoparticles $k_{Brownian}$:Thermal conductivity enhancement due to the effect of Brownian motion γ: Modeling parameter, refers to the hydrodynamic interaction among the Brownian motion induced (moving) fluid	[58]

Table 4
Physical characteristics of ethylene glycol, water, and MWCNTs.

	Density, kg/m^3	Specific heat, J/kg °C	Thermal conductivity, W/m °C	Ref.
MWCNTs	2100	720	0.6–6600	[59]
Water	998	4187	0.63	
Ethylene glycol	1038.4	3750	0.25	[60]

2.4. Preparation of nanofluid

Two types of nanofluids were synthesized namely, multi-walled carbon nanotubes/water and/ethylene glycol through two stages: (i) steric stabilization and (ii) sonication. The base fluid was prepared by mixing distilled water with sodium dodecyl benzene sulfonate (SDBS) as a surfactant at 1300 r.p.m for 40 min using a magnetic stirrer. Then, different loadings of MWCNTs were dispersed in the solution of DW-SDBS. For good mixing stability, it was reported that ratio of carbon nanotubes to SDBS surfactant is 2:1 [61]. Carbon nanotubes loading was 1 % (wt./wt.) in MWCNTs/water and MWCNTs/ethylene glycol nanofluids.

If the nanoparticles in the nanofluid aggregate or settle out of the fluid, they can clog the cooling system, reduce heat transfer efficiency, and even damage pipelines. Moreover, the instability of nanofluids can lead to inconsistent heating performance, making it difficult to predict and control the heating process. Therefore, ultrasonic processor for an additional 2 h to produce stable dispersed surfactant MWCNTs/water and MWCNTs/ethylene glycol nanofluids was applied. By improving nanofluid stability, the heating efficiency of nanofluids can be enhanced, making them a promising option for solar collector's applications. Using a magnetic stirrer, the nanofluid was extensively mixed to maintain stability and avoid agglomeration. Nanofluid was then sonicated using an ultrasonic processor for an additional 2 h to produce stable dispersed surfactant MWCNTs/water and MWCNTs/ethylene glycol nanofluids. Ratios of MWCNTs to water and ethylene glycol were calculated by eq. (4).

$$\%\text{Vol. loading}, \varphi = (W_s/\rho_s) / \left[(W_s/\rho_s) + (W_f/\rho_s)\right] \quad (3)$$

where W_p and p are the weight and density of nanoparticles, respectively, and W_{bf} is the weight of base fluid.

2.5. Nanofluids characteristics

Synthesized nanofluids MWCNTs/water and MWCNTs/ethylene glycol were analyzed using the laser-light scattering method for measuring size distribution of the used MWCNTs and zeta potential (Malvern Zetasizer Nano ZS90) for measuring fluid stability. The distribution of MWCNTs in water and ethylene glycol are listed in Table 5.

Table 5
Particles sizes and Zeta potentials of MWCNTs/water and MWCNTs/Ethylene glycol nanofluids at $\varphi = 0.57$

	Primary specified particle size (nm)	Secondary particle size (nm)	Particle size ratio	Zeta potential (mV)
MWCNTs/water/SDBS	14.32	1383	96.57	−108.7
MWCNTs/Ethylene glycol/SDBS	13.95	100	97.16	−105.3
MWCNTs/water	27.10	1420	90.2	−30
MWCNTs/Ethylene glycol	21.9	210	83.1	−27

In the nanofluids of MWCNTs/water and MWCNTs/ethylene glycol, the average particle size of the MWCNTs is in water and ethylene glycol is 16.8 nm and 10.7 nm respectively as shown in Figs. 2 and 3. The assessment of size distribution by intensity in water-based nanofluid revealed the presence of dual peaks, measuring 14.32 nm (peak 1) and 1383 nm (peak 2) with a particle size ratio of 96.57:3.43. In contrast, the ethylene glycol nanofluid exhibited peaks at 13.95 nm (peak 1) and 100 nm (peak 2) with a particle size ratio of 92.84:7.16. Multi-walled carbon nanotubes (MWCNTs) have a tendency to aggregate or clump together when exposed to water or other polar solvents. This is due to the fact that MWCNTs are hydrophobic in nature and prefer to interact with other hydrophobic surfaces rather than water. This tendency to aggregate can have negative effects on the properties of MWCNTs, such as reducing their dispersibility and increasing their tendency to form non-uniform coatings or films. In ethylene glycol, charged MWCNTs can repel each other, resulting in a larger hydrodynamic radius and apparent particle size. Similarly, surfactant SDBS can coat the particles and increase their effective size, leading to larger size measurements of MWCNTs in ethylene glycol. The measurement of zeta potential is one of the most commonly used tests to evaluate the stability of nanofluid. Zeta potential is a measure of the electrostatic repulsion between particles in a suspension and is a key factor in determining the stability of the nanofluid. In Table 5, high negatively charged of MWCNTs in water and ethylene glycol −108.7 mV and −105.3 mV indicated that the MWCNTs were well-dispersed and repelled each other, resulting in a stable suspension [62].

3. Performance evaluation of solar collector

The thermal efficiency (η_{th}) of a solar collector can be defined as the ratio between the actual useful energy gained by the heat transfer fluid, typically water (Q_U), and the incident solar radiation on the absorber of the solar collector. This can be mathematically expressed by equation (5) [62–64].

$$\eta_{th} = \frac{Q_U}{G\Delta T A_{sc}} \quad (4)$$

The actual useful energy (Q_U) denotes the energy acquired by the heat transfer fluid (e.g., water) from the solar collector, encompassing the energy effectively collected and used for specific purposes, such as water heating. The effective area (A_{sc}) refers to the absorber's surface area actively engaged in absorbing solar radiation, accounting for any shading or design inefficiencies in the collector. Solar radiation (G) represents the solar energy incident per unit area on the collector's surface, influenced by factors like geographical location, time of year, and collector orientation. Change in temperature (ΔT) signifies the variance in temperature between the collector's absorber and the surrounding environment, playing a crucial role in determining the heat transfer to the working fluid.

The actual useful energy (Q_U) in Watt unit obtained from the solar collector could be determined by the following equation:

$$Q_U = m_f C_p (T_o - T_i) \quad (5)$$

The energy stored (Q_S) in Joule unit is computed by using equation (7):

$$Q_S = MC_p (T_a - T_b) \quad (6)$$

where, A: Area of the collector in square meters (m^2). This refers to the surface area of the collector that is exposed to solar radiation. Cp: Specific heat capacity of water, approximately equal to 4187 J kg^{-1}) K^{-1}. This is the amount of heat energy required to raise the temperature of water by 1 K per unit mass, I: Intensity of solar radiation in watts per square meter (W/m^2). It represents the amount of solar energy received per unit area. M: Mass of water in the storage tank in kilograms (kg). This refers to the total mass of water present in the tank. m_f: Mass flow

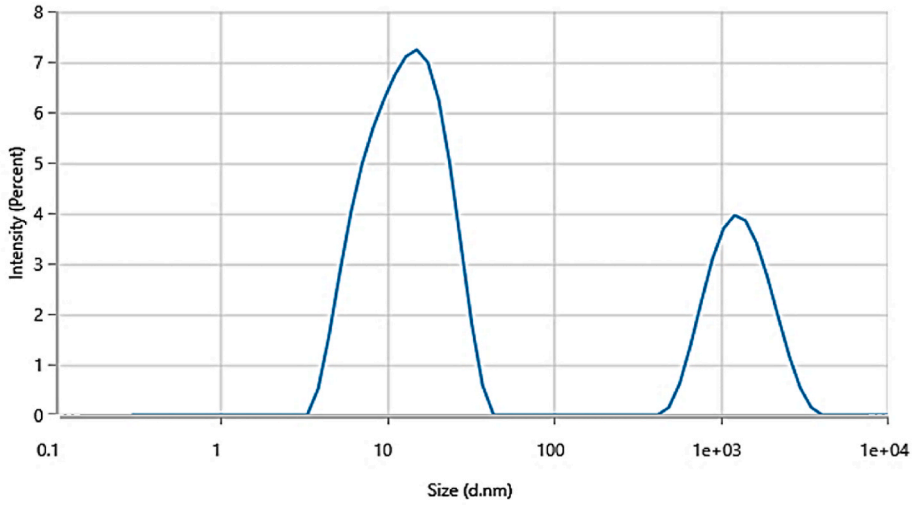


Fig. 2. Zeta sizer of the prepared SDBS - MWCNTs/water nanofluid.

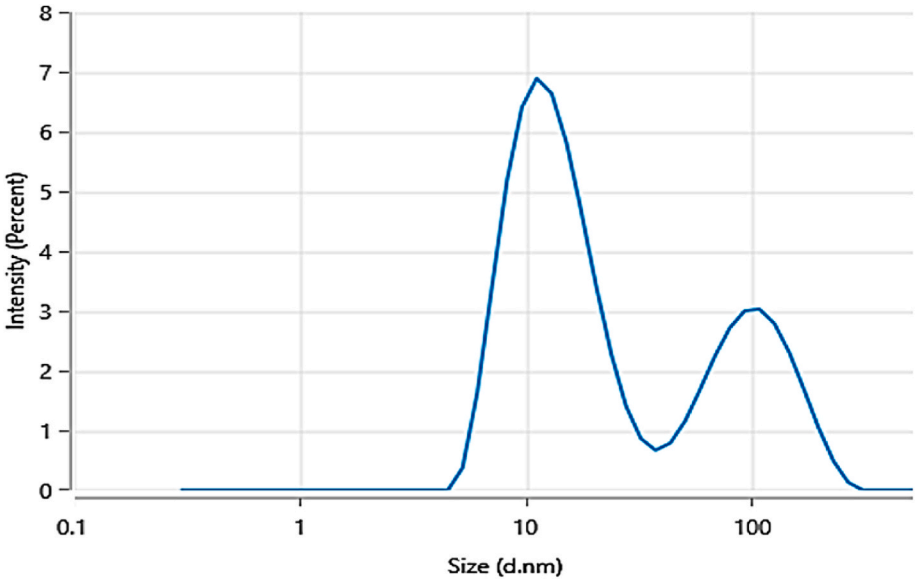


Fig. 3. Zeta sizer of the prepared SDBS - MWCNTs/ethylene glycol nanofluid.

rate of water in kilograms per second (kg/s). It represents the amount of water flowing through the system per unit time. T_i: Inlet temperature of water in degrees Celsius (°C). It indicates the initial temperature of the inlet water entering the collector. T_o: Outlet temperature of water in degrees Celsius (°C). It represents the final temperature of the water leaving the collector. T_a: Initial temperature of the water in degrees Celsius (°C). This refers to the initial temperature of the water in the storage tank. T_b: Final temperature of the water in degrees Celsius (°C). It refers to the final temperature of the water in the storage tank. These variables were used to describe and calculate various parameters related to the heat transfer and energy balance in the system.

4. Results and discussion

The experiments were performed in the ambient environmental conditions to compare FPSC and PTSC using nanofluid and study its effect on the residential SWH system performance at variable flow rates (m_f). The different temperatures were measured during 8 h from 8:00 a.m. to 16:00 p.m. All average measurements were taken during the month of July. It is worth mentioning that FPSC gave outstanding outcomes compared with the PTSC in terms of thermal efficiency (η_{th}), useful energy gain (Q_U), stored energy (Q_S), outlet hot water temperature (T_o) and the temperature difference (ΔT) at all examined m_f of 0.47, 1.05 and 1.75 kg min^{-1}

4.1. Measurements at variable mass flow rate

The resulting measurements illustrates the hourly variation of the solar radiation intensity (I), ambient air temperature (T_a) and hot outlet water temperature (T_o) with time in sunny days. I and T_a are independent of flow rate (m_f) and solar collector kind. Fig. 4(A, B and C) shows that the I and T_a both increased remarkably from sunrise solar time till the peak at noon solar time, then declined notably until reached to the minimal value at the evening hours. The data of I and T_a were measured per hour and average values were reported as follows: (644 W m^{-2} and 26.6 °C), (548.2 W m^{-2} and 27.7 °C) and (700 W m^{-2} and 27.4 °C) for the two investigated FPSC and PTSC at different m_f of 0.47, 1.05 and 1.75 kg min^{-1}, respectively.

Unlike I and T_a, the T_o was found to be dependent on flow rate (m_f) and the type of solar collector used. The maximum possible T_o values

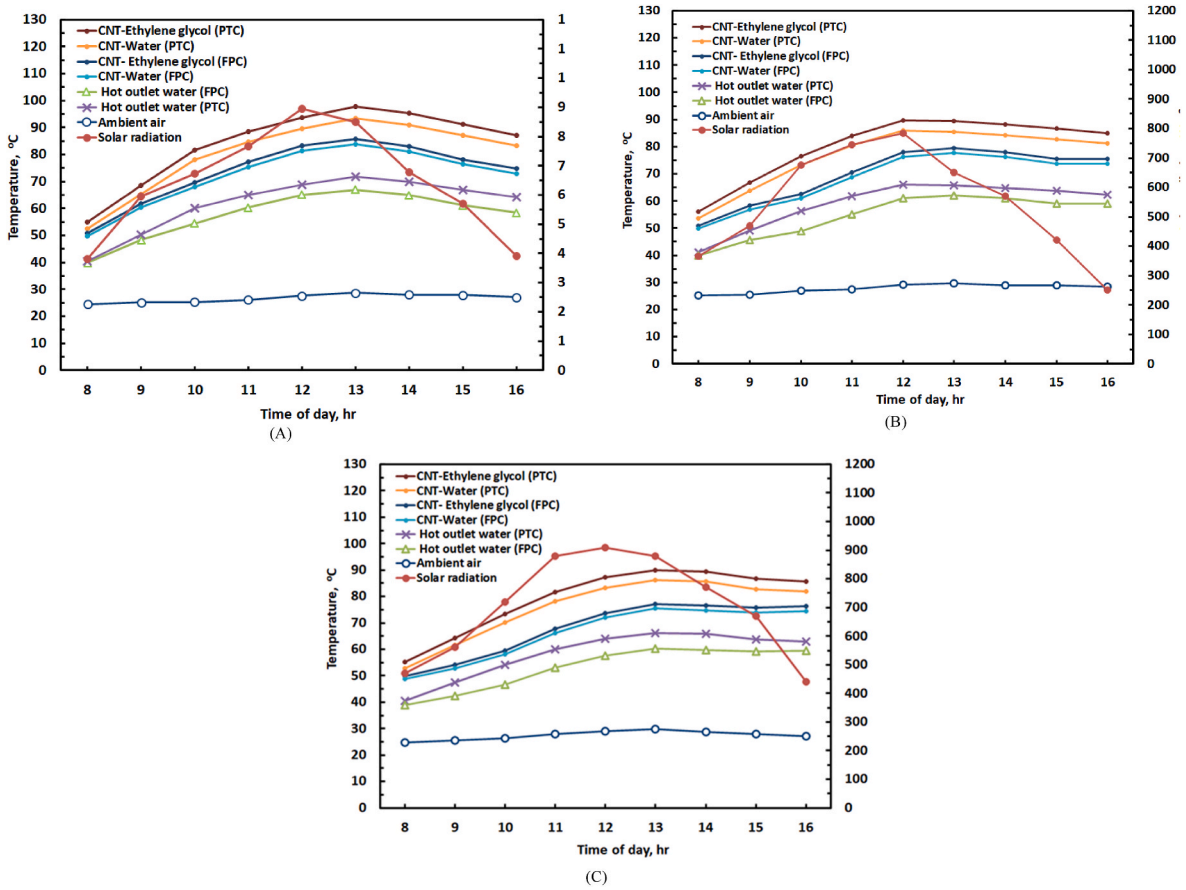


Fig. 4. Temperature and solar radiation intensity variation with solar time. (A) Temperature and solar radiation using different nanofluids using flow rate (0.47 kg min^{-1}). (B) Temperature and solar radiation using different nanofluids using flow rate (1.05 kg min^{-1}**).** (C) Temperature and solar radiation using different nanofluids using flow rate (1.75 kg min^{-1}).

were resulted at 12:00 p.m., 13:00 p.m. and 14:00 p.m. solar times for FPSC and PTSC both as illustrated in Fig. 4 (A, B and C). It was perceived from the experimental outcomes that the average T_o decreases as the m_f increases for FPSC and PTSC both. However, the solar collector type plays an important role in determining the T_o value. The PTSC is more influential than FPSC in elevating the average T_o as elaborated in Fig. 4 (A, B and C). In the case of using water only, the PTSC considerably incremented the average T_o around 61.9 °C, 58.9 °C and 58.3 °C corresponding to augmentations only up to 57.7 °C, 54.5 °C and 52.9 °C for FPSC case at m_f of 0.47, 1.05, and 1.75 kg min^{-1}, respectively. Özcan et al. [26] translated this remarked enhancement to the concentrated incident solar radiation on the absorber which resulted in a high temperature degree on the outside copper absorber surface. Therefore, heat is transferred from copper absorber tube to the water flowing through it, thus the hot outlet water temperature (T_o) increments. Similarly, in case of using CNT-water, the average T_o of the PTSC was improved significantly to about 80.5 °C, 76.7 °C and 75.8 °C corresponding to increases only up to 72.1 °C, 68.2 °C and 66.2 °C for the FPSC case at m_f of 0.47, 1.05, and 1.75 kg min^{-1}, respectively. Also, it is evident from Fig. 4(A, B and C) that the average T_o of PTSC was incremented extremely about 84.3 °C, 80.2 °C and 79.3 °C by virtue of CNT-Ethylene glycol compared with the FPSC case (i.e., 73.9 °C, 69.9 °C and 67.8 °C) at m_f of 0.47, 1.05, and 1.75 kg min^{-1}, respectively. It was noticed that there is a remarkable increase in (To) in the presence of CNTs. Carbon nanotubes are made of carbon atoms arranged in a cylindrical shape and have a very high aspect ratio, which means that they are very long and thin. This unique structure gave them exceptional thermal conductivity, which can be up to 10 times higher than that of copper. When CNTs were added to the working fluid in a solar collector, they formed a network that increased the thermal conductivity of the fluid. This network of CNTs can also act as a nucleation site for the formation of bubbles, which enhanced heat transfer by creating turbulence and promoting mixing in the fluid.

4.2. The variation of temperature difference (ΔT) at variable mass flow rate

The study investigated the variation of temperature difference (ΔT) between the cold inlet and hot outlet water over hourly time intervals during the process. The investigation compared two types of collectors; FPSC and PTSC. Fig. 5(A, B and C) shows that the temperature difference (ΔT) generally increased from the morning hours and reached its maximum value around the afternoon. Afterward, ΔT gradually declined during the evening hours. This pattern indicated that the temperature difference between the inlet and outlet water was highest when the solar radiation and heat input were at their peak. Figure (5, A, B, and C), likely presents the relationship between mass flow rate (m_f) and the temperature difference (ΔT). The description indicated that as the mass flow rate increased, the temperature difference (ΔT) decreased. This inverse relationship implied that higher flow rates resulted in a reduced temperature difference between the inlet and outlet water.

It is clear that as m_f increased, the ΔT gradually decreased independent of solar collector kind. Özcan et al. [26] explained the obtained result as the quantity of heat transferred per unit volume of water was kept at a lower level for a higher m_f through the collector, hence decreasing the ΔT. The obtained results are in a good agreement with the findings reported by Bolaji [65]. They show that in case of utilizing pure water, the PTSC greatly increased the average ΔT to about 11.8 °C,

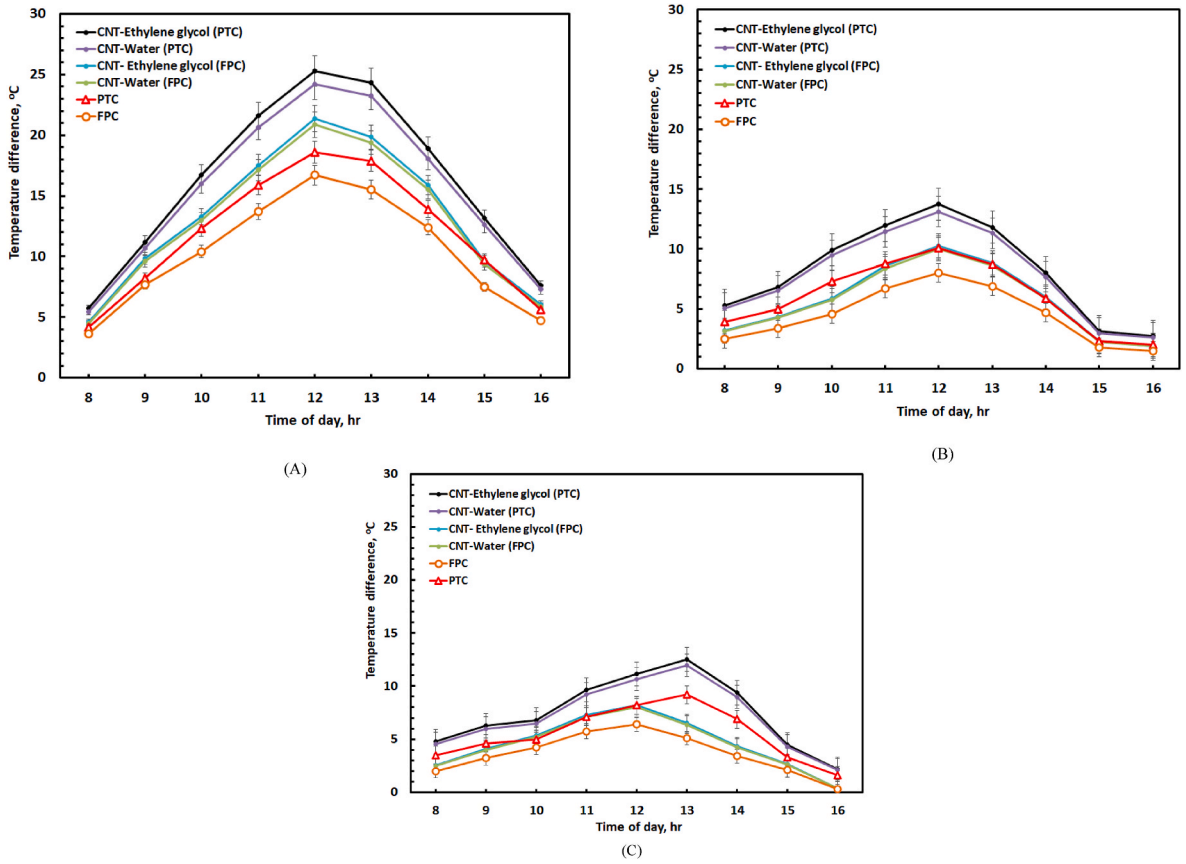


Fig. 5. Hourly temperature difference between cold inlet and hot outlet water collector as a function of solar time for the considered solar collectors. (A) Temperature difference (ΔT) vs. time at flow rate (0.47 kg min^{-1}) of different collectors. (B) Temperature difference (ΔT) vs. time at flow rate 1.05 kg min^{-1} of different collectors. (C) Temperature difference (ΔT) vs. time at flow rate 1.75 (kg min^{-1}) of different collectors.

6 °C and 5.5 °C while they increased up to 10.2 °C, 4.4 °C and 3.6 °C in case of FPSC at m_f of 0.47, 1.05 and 1.75 kg min^{-1}, respectively. Boosting the ΔT by around 15.7 %, 36.4 % and 52.8 % can be attributed to the vital role of PTSC in concentrating of incident solar radiation by using a reflector. FPSC showed increase in the average collector hot outlet water temperature (T_o) by 7.3 %, 8.1 % and 10.2 % at m_f of 0.47, 1.05, and 1.75 kg min^{-1}, respectively. It was noticed from the experimental results presented in Fig. 5(A, B and C) that the CNT-ethylene glycol enhanced remarkably the average ΔT of the parabolic trough collector (PTC) to approximately 25.1 °C, 14.2 °C and 13.1 °C. Carbon nanotube nanofluid improved the heat transfer efficiency and increase the temperature difference between the absorber tube and the working fluid. This led to higher thermal efficiencies and improved performance of the collector. In flat plate collector (FPC) system, carbon nanotubes-ethylene glycol improved ΔT to 21.2 °C, 9.8 °C and 7.1 °C at m_f of 0.47, 1.05 and 1.75 kg min^{-1}, respectively as illustrated in Fig. 5 (A, B and C). Increasing the mass flow rate of nanofluid in a heat transfer system from 0.47 kg min^{-1} to 1.75 kg min^{-1} led to a decrease in the temperature difference between the hot and cold fluids. This is because reducing the flow rate allowed less time for the heat transfer to occur between the two fluids, resulting in a lower temperature difference between them.

4.3. Stored and useful energy gain at variable mass flow rates

Figure (6) illustrates the change in the amount of stored energy (Q_S) in FPC and PTC. Experiments were implemented at diverse m_f of 0.47, 1.05 and 1.75 kg min^{-1}. In the PTC and FBC, stored energy (Qs) increased significantly up to 4.49 MJ, 1.50 MJ and 1.40 MJ at m_f of 0.47, 1.05 and 1.75 kg min^{-1}, respectively. A parabolic trough collector (PTC)

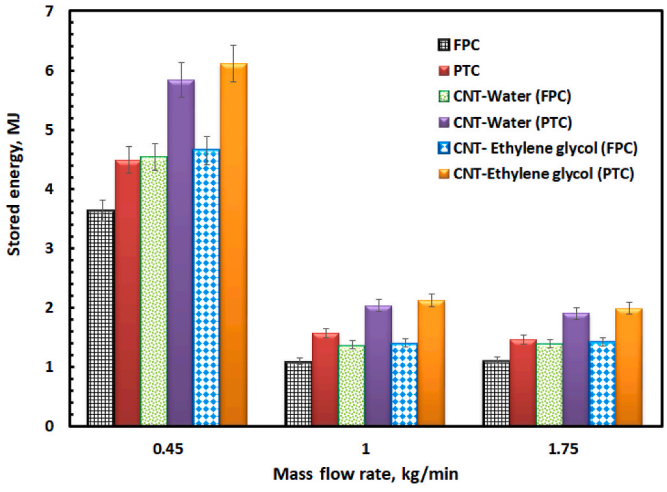


Fig. 6. The average stored energy for the considered solar collectors at different flow rates.

showed a higher potential to store more thermal energy than a flat plate collector (FPC), primarily due to its higher concentration ratio and higher operating temperatures. A parabolic trough solar collector uses a parabolic-shaped mirror to focus sunlight onto a receiver tube located at the focal point of the mirror. The receiver tube contained a heat transfer fluid that absorbed the concentrated solar radiation and was heated to high temperatures. The heated fluid was then used to generate steam or heat a thermal storage system for later use. In contrast, a flat plate solar

collector typically operated at lower temperatures, and was less efficient at capturing and storing solar energy. This is because the flat plate collector has a lower concentration ratio and a larger surface area than the parabolic trough collector, which reduced its ability to concentrate and capture solar radiation. It was also found that the Q_S is adversely proportional to the m_f, whereas the Q_S in MJ units increases as the m_f decreases for both investigated PSC and FPC. In PSC, maximum Q_S was 4.49 MJ at the lowest m_f of 0.47 kg min^{-1}. It can be noticed from Figure (6) that CNT-Water increased significantly the amount of stored energy (Q_S) of the PTSC 28.6 %, 48.2 % and 36.7 % in comparison FPC at m_f of 0.47, 1.05 and 1.75 kg min^{-1}, respectively. Similarly, amount of stored energy (Q_S) of the PTSC was enhanced extremely by about 31.4 %, 51.4 % and 39.4 % in the presence of CNT-ethylene glycol at m_f of 0.47, 1.05 and 1.75 kg min^{-1}, respectively.

The use of nanofluids showed potentially increase the amount of thermal energy that can be stored, due to their enhanced thermal properties. Nanofluids exhibited higher thermal conductivity and specific heat capacity than water and ethylene glycol fluid alone. When used as a heat transfer fluid in a solar collector, nanofluids increased the amount of thermal energy that is absorbed and transferred to a storage medium. This is because the CNTs in the nanofluid enhanced the convective heat transfer between the collector and the fluid, leading to more efficient heat transfer and higher overall thermal efficiency. In addition, CNTs nanofluids also increased the thermal energy storage capacity of a solar collector, since they have higher specific heat capacity than the base fluid. This means that a given volume of CNTs nanofluid can store more thermal energy than the same volume of pure fluid.

Useful energy gain (Q_U) increased significantly from FPSC to PTSC at various m_f of 0.47, 1.05 and 1.75 kg min^{-1} as shown in Figure (7). The CNTs-water showed high useful energy gain (Q_U) up to 21.6 %, 32.5 % and 23 % from FPSCs to PTSCs at different m_f of 0.47, 1.05 and 1.75 kg min^{-1}, respectively. Similarly, it was found that the CNT-ethylene glycol enhanced notably the value of Q_U by about 24.3 %, 35.3 % and 25.7 % from FPSCs to PTSCs.

Unlike the Q_S, the Q_U was directly proportional to m_f whereas the Q_U in KW units increased as the m_f increased. The useful gain energy in FPC and PTC increased at high mass flow rate due to several factors: (i) A higher mass flow rate increased the convective heat transfer coefficient between the absorber surface and the working fluid, leading to more efficient heat transfer and higher overall thermal efficiency. This is because a higher mass flow rate can help to overcome the thermal resistance of the boundary layer near the absorber surface, which can limit the rate of heat transfer at low flow rates, and (ii) A higher mass flow rate can help to reduce the temperature of the working fluid and limit its temperature rise across the collector, which can help to prevent thermal degradation of the working fluid and improve its longevity.

Parabolic trough solar collector (PTSC) showed maximum Q_U 38 KW, 49.4 KW and 51.7 KW at high mass flow rate (m_f) 1.75 kg min^{-1} in the presence of water, CNT-Water and CNT-ethylene glycol, respectively. Ethylene glycol has a lower specific heat capacity and thermal conductivity compared to water, which resulted in lower thermal efficiency and lower useful gain in energy in solar collectors. These findings are in a good agreement with reported results [26].

4.4. Thermal efficiency at various mass flow rates

Figure (8) displays the impact of varying m_f on the η_{th} of the two investigated solar collectors (*i.e.,* FPSC and PTSC). It was found that increasing m_f from 0.47 to 1.75 kg min^{-1} improved significantly the η_{th}. Similar results were reported by Özcan et al. [26] and Alvarez et al. [79]. Moreover, Figure (8) shows also the comparison outcomes between the FPSC and PTSC impact on the residential SWH system performance regarding the η_{th}. Experimental comparison outcomes proclaimed that the average η_{th} increased to 37 %, 45.7 % and 59.2 % in case of PTSC at different m_f 0.47, 1.05, and 1.75 kg min^{-1}, respectively. The rate of increasing was around 1.18, 1.27 and 1.18 times from FPSC to PTSC at different m_f of 0.47, 1.05 and 1.75 kg min^{-1}, respectively. In case of CNT-water, the average η_{th} greatly increased to around 48.1 %, 59.4 % and 77 % in case of PTSC at different m_f of 0.47, 1.05, and 1.75 kg min^{-1}, respectively. The rate of increase was 1.23, 1.32 and 1.23 times from FPSC to PTSC at different m_f of 0.47, 1.05 and 1.75 kg min^{-1}, respectively. In case of CNT-ethylene glycol, the average η_{th} greatly increased up to 50.3 %, 62.1 % and 80.6 % in PTSC system at different m_f of 0.47, 1.05, and 1.75 kg min^{-1}, respectively. The rate of increasing was approximately 1.25, 1.35 and 1.25 times from FPSC to PTSC at different m_f of 0.47, 1.05 and 1.75 kg min^{-1}, respectively. This improvement can be attributed to elevating the average T_o as a result of the positive PTSC effect in concentrating more incident solar radiation comparing to FPSC which in turn enlarged the ΔT and improved the η_{th}. The improvements of thermal efficiency are listed in Table 6. Remarkable enhancement was found using MWCNTs in the presence of sodium dodecyl benzene sulfonate (SDBS) comparing with other nanoparticles.

In the tested range of m_f under the prevailing weather conditions, Fig. 9 (A, B and C) shows the variation of η_{th} with hourly time. It is obvious that the η_{th} of FPSC and PTSC were generally boosted at the beginning of the day until reached to the greatest value at noon hour, then gradually decreased to the lowest value at afternoon hours. The

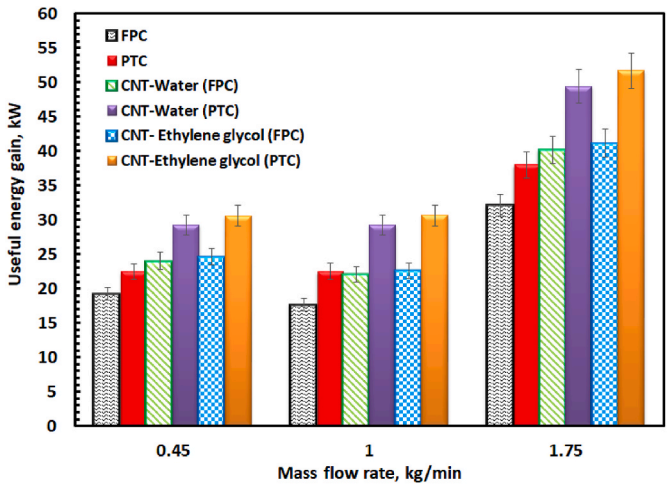


Fig. 7. The average useful energy gain for the considered solar collectors at different flow rates.

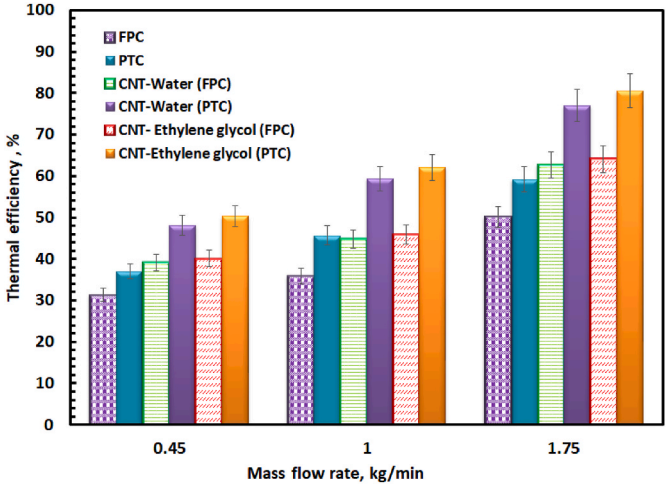
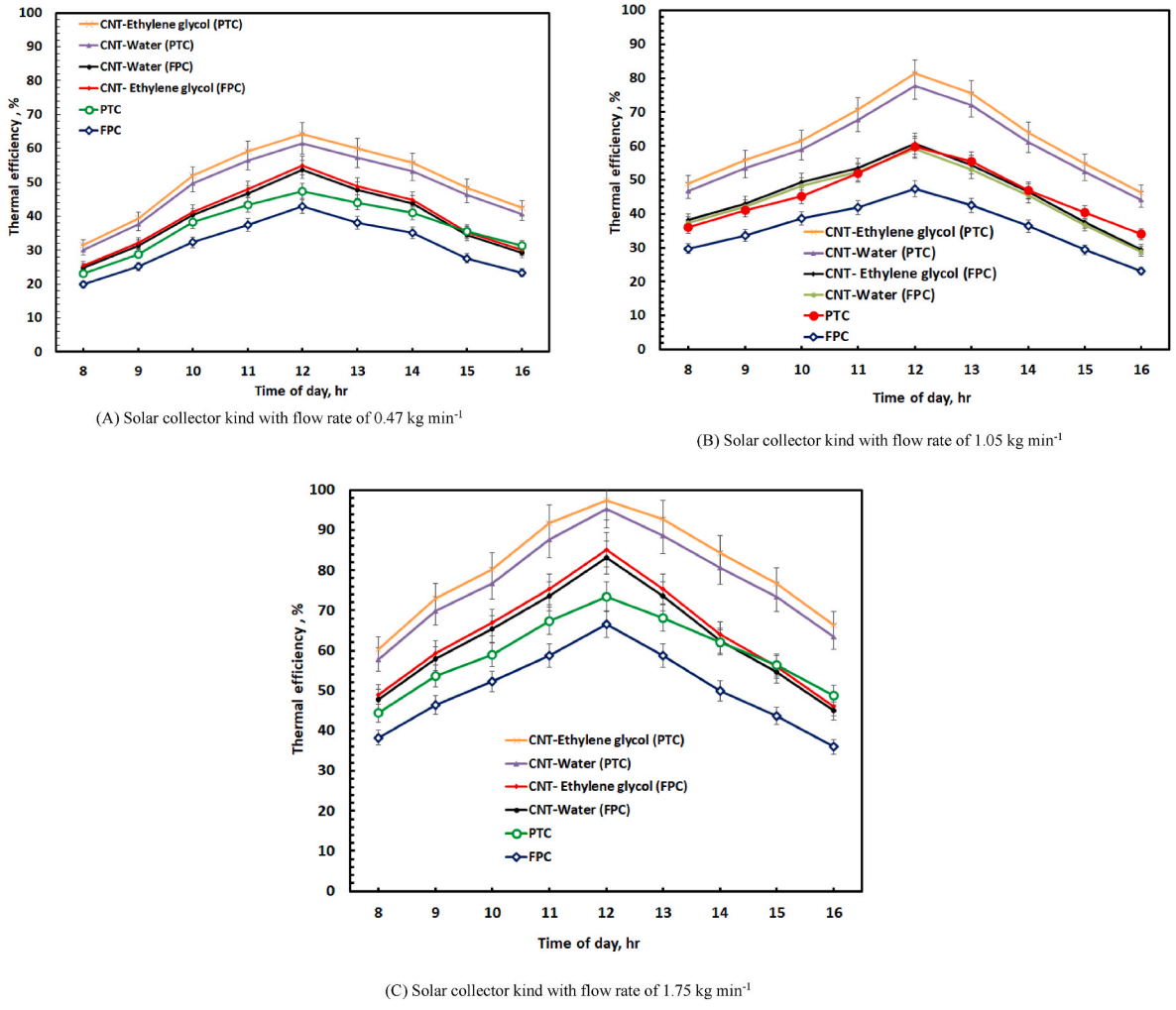


Fig. 8. The average thermal efficiency for the considered solar collectors and different flow rates.

Table 6
Thermal performance of nanofluids.

Research study	Nanofluid	Type of solar collector	Volume concentration (%)	Thermal efficiency enhancement (%)	Ref.
Mouli et al.	MWCNT/Water	Flat plate	0.3	52.4	[66]
Singh et al.	Al_2O_3-water	Flat plate	0.2	28.47	[67]
Zafar et al.	MWCNT-Fe_3O_4/water	Flat plate	0.05–0.3	52.15–63.83	[68]
Faizal et al.	SiO_2-water	Flat plate	0.2	23.50	[69]
Farajzadeh et al.	Al_2O_3–TiO_2/water	Flat plate	0.1	21–26	[70]
Ghasemi et al.	CuO-water	Parabolic trough	3	35	[71]
Alejandro et al.	Al_2O_3/water	Parabolic trough	1–3	57.7	[72]
Kasaeian et al.	MCNT/mineral oil	Parabolic trough	0.2 %–0.3 %	5–7	[73]
Tiwari et al.	MWCNT and Nano silica/EG	Parabolic trough	0.0–0.6	80.7 and 70.9	[74]
Heyhat, M. M. et al.	nanofluid, metal foam	Parabolic trough	0.1	55.65–79.29	[75]
Kanti et al.	Al_2O_3-water	Flat plate	0–1	76.3	[76]
Menbari et al.	Al_2O_3–CuO/water	Parabolic trough	0.05–2	48	[77]
Arani. and Monfaredi	SiC/EG-water	Parabolic trough	4 %	30	[78]
In this study	MWCNTs -water	parabolic trough	1 %	77	
	MWCNTs -ethykene glycol	Parabolic trough	1 %	80	
	MWCNTs -water	Flat plate	1 %	63	
	MWCNTs -ethykene glycol	Flat plate	1 %	64	



(A) Solar collector kind with flow rate of 0.47 kg min^{-1}

(B) Solar collector kind with flow rate of 1.05 kg min^{-1}

(C) Solar collector kind with flow rate of 1.75 kg min^{-1}

Fig. 9. Hourly thermal efficiency variation with a solar time for the considered solar collectors and different flow rates. (A) Solar collector kind with flow rate of 0.47 kg min^{-1} (B) Solar collector kind with flow rate of 1.05 kg min^{-1} (C) Solar collector kind with flow rate of 1.75 kg min^{-1}.

lowest recorded η_{th} value at the beginning of the day and afternoon hours could be ascribed commonly to the limited solar radiation intensity at these times. While, the highest recorded η_{th} value at noon time attributed to the ΔT increase.

4.5. Possibility of carbon dioxide emissions mitigation

Struggling with the consequence of global warming brought on by huge CO_2 releases has emerged as one of the most challenging issues confronting human civilization [80]. For example, the production of power from fossil fuels results in the creation of several pollutants, the

most dangerous of which being CO_2, as well as SO_2 and NOX. Therefore, for efficient energy generating planning, decreasing pollution in the electricity industry is essential [81]. Solar collectors are among the renewable energy products with the greatest average growth rate. Along with being renewable, solar collectors' technology has the benefit of being clean. The next formula could be utilized to calculate the total CO_2 releases saved by the solar collector system [82].

$$m_t = m_e \; x \; dE \; x \; t_{life} \tag{7}$$

where mt is the whole reduced CO_2 (g) emission quantity through its lifecycle, me is the mean emission intensity of CO_2 (904 g/kWh) by a power plant working with coal-fired [83]. dE is the whole day energy reduction of the FPSCs/PTSCs systems (kWh/day), and tlife is the cost-effective lifespan of the FPSCs/PTSCs systems which can be assumed as 20 years [84].

Solar intensity values for the day were 6.3 kW/day is shown in Fig. 10. The production of useful thermal energy gain was influenced significantly by solar intensity. The accumulated useful thermal energy gain reached 34.5 kW/m^3day and 43.45 kW/m^3day for FPSCs and PTSCs system, respectively. The results showed a significant decrease in CO_2 releases per day owing to the renewable clean power of solar collectors. The total reduction in CO_2 emissions was 31.26 kg/day and 39.28 kg/day for the FPSCs and PTSCs systems, respectively.

5. Conclusion

This study introduced a novel dimension to solar water heating through a meticulous exploration of nanofluids' influence on two prominent solar collector systems. By showcasing substantial advancements in thermal efficiency and significant reductions in CO_2 emissions. The outcomes of this research work demonstrated that the utilization of a parabolic trough solar collector (PTSC) achieved a significant improvement in the performance of residential SWH system. The PTSC performance was evaluated and compared with the FPSC including thermal efficiency (η_{th}), useful energy gain (Q_U), stored energy (Q_S), outlet hot water temperature (T_o) and temperature difference (ΔT) at different flow rates (m_f) of 0.47, 1.05 and 1.75 kg min^{-1}. The findings of the present study showed that (i) In PTSC, the average hot outlet water temperature (T_o) was around 61.9 °C, 58.9 °C and 58.3 °C. whereas the T_o was 57.7 °C, 54.5 °C and 52.9 °C in case of FPSC, (ii) In PTSC, the average temperature difference (ΔT) between the cold inlet and hot outlet water increased up to 11.8 °C, 6 °C and 5.5 °C whereas it increased to 10.2 °C, 4.4 °C and 3.6 °C in FPSC, (iii) In PTSC, the temperature of 120-L increased up to 59.1 °C, 56.1 °C and 55.7 °C, respectively within 8 h of sunshine whereas it increased only up to 54.7 °C, 52.3 °C and 51.6 °C in FPSC, (iv) The average thermal efficiency (η_{th}) was enhanced up to 28 % and 36 % in the presence of ethylene glycol nanofluid using PTSC and FPSC respectively (v) A significant saving in CO_2 release per season is owing to the renewable clean energy of solar collectors. The total reduction in CO_2 emissions was 31.26 kg/day and 39.28 kg/day for the FPSCs and PTSCs systems, respectively. Based on the obtained outstanding outcomes, the designed parabolic trough solar collector (PTSC) in the presence of MWCNTs nanofluid was trustworthy and reliable and met the demands of residential, agricultural and industrial process in terms of giving high hot outlet water temperature and thermal efficiency. This research not only pushes the boundaries of SWH technology but also contributes meaningfully to the transition towards cleaner and more sustainable energy solutions.

Funding

Not Applicable.

CRediT authorship contribution statement

Mostafa AbdEl-Rady Abu-Zeid: Writing - review & editing, Writing - original draft, Resources, Methodology, Investigation, Formal analysis, Data curation, Conceptualization. **Yasser Elhenawy:** Writing - review & editing, Writing - original draft, Visualization, Resources, Methodology, Investigation, Formal analysis, Data curation, Conceptualization. **Mohamed Bassyouni:** Writing - review & editing, Writing - original draft, Visualization, Validation, Resources, Methodology, Investigation, Formal analysis, Conceptualization. **Thokozani Majozi:** Writing - review & editing, Methodology, Conceptualization. **Monica Toderaș:** Writing - review & editing, Writing - original draft, Visualization, Validation, Resources, Methodology, Investigation, Formal analysis, Conceptualization. **O.A. Al-Qabandi:** Writing - review & editing, Writing – original draft, Visualization, Resources, Methodology, Investigation, Formal analysis, Conceptualization. **Sameh Said Kishk:** Writing - review & editing, Writing - original draft, Visualization, Validation, Resources, Methodology, Investigation, Formal analysis, Data curation, Conceptualization.

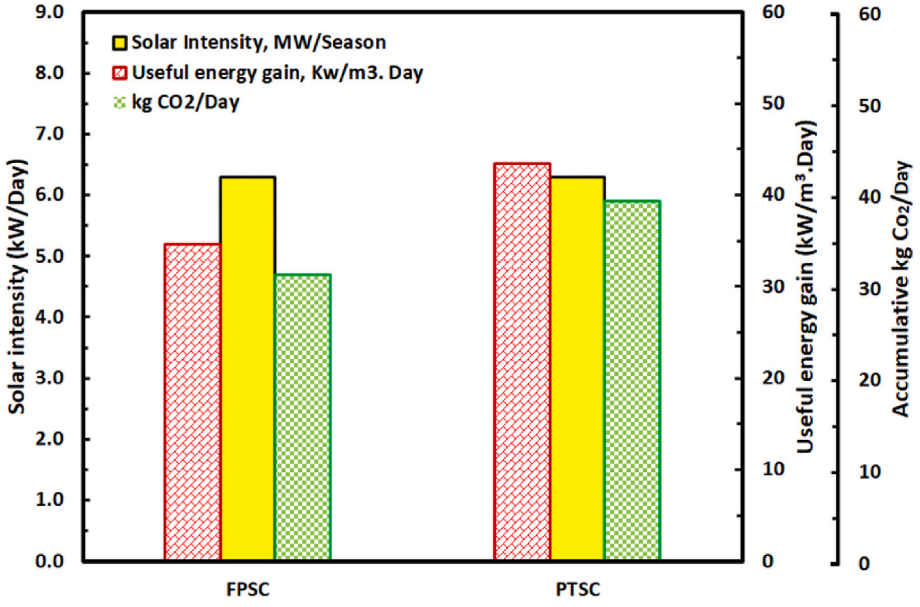


Fig. 10. Demonstrates the daily freshwater harvest, CO_2 emissions reduction, and total solar intensity of various solar collecting systems.

Declaration of competing interest

The authors declare that they have no known competing financial interests or personal relationships that could have appeared to influence the work reported in this paper.

Data availability

Data will be made available on request.

Acknowledgments

The researchers would like to acknowledge the assistance provided by the Science and Technology Development Fund (STDF) for funding the project, No. 41902 (Center of Excellence in Membrane-based Water Desalination Technology for Testing and Characterization".

Nomenclature

FPSC	Flat-plate solar collector
PTSC	Parabolic trough solar collector
SWH	Solar water heating
A	Solar collector area (m^2)
C_P	Specific heat of water (≈4186 J kg^{-1} K^{-1})
Q_U	Useful energy gain (KW)
Q_S	Stored energy (MJ)
I	Solar radiation intensity (Wm^{-2})
M	Water Mass in storage tank (kg)
m_f	Mass flow rate (kg s^{-1})
T_o	Hot outlet water temperature (^oC)
T_a	Ambient air temperature (^oC)
T_a	Final temperature of storage tank (°C)
T_b	Initial temperature of storage tank(°C)
T_i	Inlet collector water temperature (°C)
T_o	Outlet collector water temperature (°C)
T_s	he temperature of hot water in storage tank (^oC)
ΔT	Temperature difference between cold inlet and hot outlet fluid collector (^oC)
W	Wind speed (m/sec)
η_{th}	Thermal efficiency (%)

References

[1] Sulyman O. Salawu, Adebowale M. Obalalu, Emmanuel I. Akinola, Current density and thermal propagation of electromagnetic $CoFe_2O_4$ and $TiO_2/C_2H_6O_2+H_2O$ hybridized Casson nanofluids: a concentrated solar power maximization, Results in Engineering (2023), 101200.

[2] Hani Hussain Sait, Hussain Ahmed, Bassyouni Mohamed, Imtiaz Ali, Kanthasamy Ramesh, , Bamidele Victor Ayodele, Yasser Elhenawy, Hydrogen-rich syngas and biochar production by non-catalytic valorization of date palm seeds, Energies 15 (8) (2022) 2727.

[3] Yasser Elhenawy, Bassyouni Mohamed, Kareem Fouad, , Abdelfatah Marni Sandid, Mostafa Abd El-Rady Abu-Zeid, Thokozani Majozi, Experimental and numerical simulation of solar membrane distillation and humidification–dehumidification water desalination system, Renew. Energy 215 (2023), 118915.

[4] A.S. Abdullah, Hitesh Panchal, Wissam H. Alawee, Z.M. Omara, Methods used to improve solar still performance with generated turbulence for water desalination-detailed review, Results in Engineering (2023), 101251.

[5] Y. Elhenawy, G.H. Moustafa, , Attia Mahmoud Attia, A.E. Mansi, Thokozani Majozi, M. Bassyouni, Performance enhancement of a hybrid multi effect evaporation/membrane distillation system driven by solar energy for desalination, J. Environ. Chem. Eng. 10 (6) (2022), 108855.

[6] Mashrur Muntasir Nuhash, Md Ibthisum Alam, Ananta Zihad, Md Jahid Hasan, Fei Duan, Arafat A. Bhuiyan, Md Rezwanul Karim, Enhancing energy harvesting performance of a flat plate solar collector through integrated carbon-based and metal-based nanofluids, Results in Engineering 19 (2023), 101276.

[7] T.K. Murtadha, A.A. Hussein, Optimization the performance of photovoltaic panels using aluminum-oxide nanofluid as cooling fluid at different concentrations and one-pass flow system, Results in Engineering 15 (2022), 100541.

[8] S.A. Kalogirou, Solar thermal collectors and applications,", Prog. Energy Combust. Sci. 30 (2004) 231–295.

[9] M.L.G. Ho, C.S. Oon, L.L. Tan, Y. Wang, Y.M. Hung, A review on nanofluids coupled with extended surfaces for heat transfer enhancement, Results in Engineering (2023), 100957.

[10] Kareem Fouad, , Mohamed Gar Alalm, Bassyouni Mohamed, Mamdouh Y. Saleh, A novel photocatalytic reactor for the extended reuse of W–TiO2 in the degradation of sulfamethazine, Chemosphere 257 (2020), 127270.

[11] G. Vishal, V. Chinmay, R. Kishor, Solar water heating systems: a review,", Int. J. Sci. Eng. Res. 3 (2015) 13–17.

[12] H. Bhowmik, R. Amin, Efficiency improvement of flat Plate collector using reflector, Energy Rep. 3 (2017) 119–123.

[13] Z. Said, M.A. Sabiha, R. Saidur, A. Hepbasli, N.A. Rahim, S. Mekhilef, T.A. Ward, Performance enhancement of a flat Plate collector using titanium dioxide nanofluid and polyethylene glycol dispersant, J. Clean. Prod. 92 (2015) 343–353.

[14] A.T. Fatigun, G.E. Adesakin, M. Gwani, Experimental determination of the effect of tube spacing on the performance of a flat plate solar collector, Int. J. Environ. Sci. 3 (1) (2012) 363–370.

[15] P.K. Mongre, B. Gupta, Experiment study of solar water heater with circulating pump and using of Aluminum tube,", Int. J. Eng. Trends Technol. 3 (2013).

[16] L.M. Ayompe, A. Duffy, Analysis of the thermal performance of a solar water heating system with flat Plate collectors in a temperate climate, Appl. Therm. Eng. 58 (Issues 1–2) (2013) 447–454.

[17] B.H. Upadhyay, A.J. Patel, P.V. Ramana, A detailed review on solar parabolic trough collector, Int. J. Ambient Energy (2019) 176–196, https://doi.org/10.1080/01430750.2019.1636869.

[18] M. Geyer, E. Lupfert, R. Osuna, A. Estebanm, W. Schiel, A. Schweitzer, Eurotrough - parabolic trough collector developed for cost efficient solar power generation, in: 11th Int. Symposium on Concentrating Solar Power and Chemical Energy Technologies, September vols. 4–6, Zurich, Switzerland, 2002.

[19] E. Elshazly, A.A. Abdel-Rehim, I. El-Mahallawi, 4E study of experimental thermal performance enhancement of flat plate solar collectors using MWCNT, Al_2O_3, and hybrid MWCNT/Al_2O_3 nanofluids, Results in Engineering 16 (2022), 100723.

[20] M. Elbany, Y. Elhenawy, Analyzing the ultimate impact of COVID-19 in Africa, Case Studies on Transport Policy 9 (2) (2021) 796–804.

[21] Y. Nada, A.A.M. Ahmed, W.M. El-Maghalany, M.R. Sohair, Absorbed solar energy in parabolic trough collector in alexandria, Egypt, Int. J. Eng. Res. Technol. 6 (11) (2017) 413–416.

[22] M. Chafie, M.F.B. Aissa, A. Guizani, Energetic end exergetic performance of a parabolic trough collector receiver: an experimental study, J. Clean. Prod. 171 (2018) 285–296.

[23] A.E. Mansi, S.M. El-Marsafy, Y. Elhenawy, M. Bassyouni, Assessing the potential and limitations of membrane-based technologies for the treatment of oilfield produced water, Alex. Eng. J. 68 (2023) 787–815.

[24] Z.D. Cheng, Y.K. Leng, J.J. Men, Numerical study on a novel parabolic trough solar receiver-reactor and a new control strategy for continuous and efficient hydrogen production, Appl. Energy 261 (2020), 114444.

[25] K. Wang, Z.D. Zhang, M.J. Li, C.H. Min, A coupled optical-thermal-fluid-mechanical analysis of parabolic trough solar receivers using supercritical CO_2 as heat transfer fluid, Appl. Therm. Eng. 183 (2021), 116154.

[26] A. Özcan, A.G. Devecioğlu, V. Oruç, Experimental and numerical analysis of a parabolic trough solar collector for water heating application, Energy Sources, Part A Recovery, Util. Environ. Eff. (2021), https://doi.org/10.1080/15567036.2021.1924317, 1–17.

[27] M. Faheem, L. Jizhan, M.W. Akram, M.U. Khan, P. Yongphet, M. Tayyab, M. Awais, Design optimization, fabrication, and performance evaluation of solar parabolic trough collector for domestic applications, Energy Sources, Part A Recovery, Util. Environ. Eff. (2020) 1–20, https://doi.org/10.1080/15567036.2020.1806407.

[28] Muhammad Zakaria, Abbas M. Sharaky, , Al-Sayed Al-Sherbini, Bassyouni Mohamed, Mashallah Rezakazemi, Yasser Elhenawy, Water desalination using solar thermal collectors enhanced by nanofluids, Chem. Eng. Technol. 45 (1) (2022) 15–25.

[29] B. Roy, S. Shovan, R.D. Balmiki, S. Das, K.P. Kataky, A. Biswasa, Parametric study of parabolic trough collector- a case study for the climatic conditions of silchar, Assam, India, ISESCO J. of Science and Technology 12 (21) (2016) 24–29.

[30] G. Rajamohan, P. Kumar, M. Anwar, T. Mohanraj, Analysis of solar water heater with parabolic dish concentrator and conical absorber, IOP Conf. Ser. Mater. Sci. Eng. 206 (2016), 29th Symposium of Malaysian Chemical Engineers (SOMChE).

[31] B.K. Hrushikesh, Design and development of prototype cylindrical parabolic solar collector for water heating application, Int. J. Renew. Energy Dev. 5 (1) (2016) 49–55.

[32] Hani Hussain Sait, Hussain Ahmed, Bassyouni Mohamed, Imtiaz Ali, Kanthasamy Ramesh, , Bamidele Victor Ayodele, Yasser Elhenawy, Anionic dye removal using a date palm seed-derived activated carbon/chitosan polymer microbead biocomposite, Polymers 14 (12) (2022) 2503.

[33] B. Bhanvase, D. Barai, Nanofluids for Heat and Mass Transfer, Elsevier, 2021.

[34] S. Akilu, A.T. Baheta, M.A. Mior, A.A. Minea, K.V. Sharma, Properties of glycerol and ethylene glycol mixture based SiO_2-CuO/C hybrid nanofluid for enhanced solar energy transport, Sol. Energy Mater. Sol. Cells 179 (2018) 118–128.

[35] F.E.B. Bioucas, S.I.C. Vieira, M.J.V. Lourenço, F.J.V. Santos, C.A. Nieto De Castro, Performance of heat transfer fluids with nanographene in a pilot solar collector, Sol. Energy 172 (2018) 171–176.

[36] Jatin Patel, Abhishek Soni, Divya P. Barai, Bharat A. Bhanvase, A minireview on nanofluids for automotive applications: current status and future perspectives, Appl. Therm. Eng. (2022), 119428.

[37] F. Didier, P. Alastuey, M. Tirado, M. Odorico, X. Deschanels, G. Toquer, Solar absorbers based on electrophoretically deposited carbon nanotubes using pyrocatechol violet as a charging agent, Thin Solid Films 764 (2023), 139614.

[38] Mashrur Muntasir Nuhash, Md Ibthisum Alam, Ananta Zihad, Md Jahid Hasan, Fei Duan, Arafat A. Bhuiyan, Md Rezwanul Karim, Enhancing energy harvesting performance of a flat plate solar collector through integrated carbon-based and metal-based nanofluids, Results in Engineering 19 (2023), 101276.

[39] S. Askari, R. Lotfi, A. Seifkordi, A.M. Rashidi, H. Koolivand, A novel approach for energy and water conservation in wet cooling towers by using MWNTs and nanoporous graphene nanofluids, Energy Convers. Manag. 109 (2016) 10–18.

[40] F. Kiliç, T. Menlik, A. Sözen, Effect of titanium dioxide/water nanofluid use on thermal performance of the flat plate solar collector, Sol. Energy 164 (2018) 101–108. .

[41] A.M. Genc, M.A. Ezan, A. Turgut, Thermal performance of a nanofluid-based flat plate solar collector: a transient numerical study, Appl. Therm. Eng. 130 (2018) 395–407. .

[42] N. Akram, E. Montazer, S.N. Kazi, M.E.M. Soudagar, W. Ahmed, M.N.M. Zubir, W. S. Sarsam, Experimental investigations of the performance of a flat-plate solar collector using carbon and metal oxides based nanofluids, Energy 227 (2021), 120452. .

[43] E.W. Bitam, Y. Demagh, A.A. Hachicha, H. Benmoussa, Y. Kabar, Numerical investigation of a novel sinusoidal tube receiver for parabolic trough technology, Appl. Energy 218 (2018) 494–510.

[44] M.R. Safaei, H. Togun, K. Vafai, S.N. Kazi, A. Badarudin, Investigation of heat transfer enhancement in a forward-facing contracting channel using FMWCNT nanofluids, Numer. Heat Tran. Part A: Appl 66 (12) (2014) 1321–1340.

[45] H. Khakrah, A. Shamloo, H.S. Kazemzadeh, Exergy analysis of parabolic trough solar collectors using Al2O3/synthetic oil nanofluid, Sol. Energy 173 (2018) 1236–1247.

[46] T. Sokhansefat, A.B. Kasaeian, F. Kowsary, Heat transfer enhancement in parabolic trough collector tube using Al2O3/synthetic oil nanofluid, Renew. Sustain. Energy Rev. 33 (2014) 636–644.

[47] I.H. Yılmaz, M.S. Söylemez, Thermo-mathematical modeling of parabolic trough collector, Energy Convers. Manag. 88 (2014) 768–784.

[48] R. Loni, E.A. Asli-Ardeh, B. Ghobadian, A. Kasaeian, Experimental study of carbon nano tube/oil nanofluid in dish concentrator using a cylindrical cavity receiver: outdoor tests, Energy Convers. Manag. 165 (2018) 593–601.

[49] M.S. Salavati, A. Kianifar, H. Niazmand, O. Mahian, S. Wongwises, Experimental investigation on the thermal efficiency and performance characteristics of a flat plate solar collector using SiO2/EG–water nanofluids, Int. Commun. Heat Mass Tran. 65 (2015) 71–75.

[50] B. Gebhart, Heat Conduction and Mass Diffusion, McGraw-Hill, Inc., New York, USA, 1993, p. 622PP.

[51] D. Huang, Z. Wu, B. Sunden, Pressure drop and convective heat transfer of Al2O3/water and MWCNT/water nanofluids in a chevron plate heat exchanger, Int. J. Heat Mass Tran. 89 (2015) 620–626. .

[52] T. Boldoo, J. Ham, H. Cho, Comparison study on photo-thermal energy conversion performance of functionalized and non-functionalized MWCNT nanofluid, Energies 12 (19) (2019) 3763.

[53] M.H. Abdel-Aziz, A.F. Al-Hossainy, A. Ibrahim, S.A. Abd El-Maksoud, M. Sh Zoromba, M. Bassyouni, S.M.S. Abdel-Hamid, A.A.I. Abd-Elmageed, I.A. Elsayed, O.M. Alqahtani, Synthesis, characterization and optical properties of multi-walled carbon nanotubes/aniline-o-anthranilic acid copolymer nanocomposite thin films, J. Mater. Sci. Mater. Electron. 29 (2018) 16702–16714.

[54] A. Melinder, Thermophysical Properties of Aqueous Solutions Used as Secondary Working Fluids, Diss. KTH, 2007.

[55] Y. Xuan, W. Roetzel, Conceptions for heat transfer correlation of nanofluids, Int. J. Heat Mass Tran. 43 (19) (2000) 3701–3707. .

[56] W. Yu, S.U.S. Choi, The role of interfacial layers in the enhanced thermal conductivity of nanofluids: a renovated Maxwell model, J. Nanoparticle Res. 5 (1–2) (2003) 167–171.

[57] Omer A. Alawi, Che Sidik Nor Azwadi, The effect of temperature and particles concentration on the determination of thermo and physical properties of SWCNT-nanorefrigerant, Int. Commun. Heat Mass Tran. 67 (2015) 8–13.

[58] J. Koo, C. Kleinstreuer, Laminar nanofluid flow in micro-heat sinks, Int. J. Heat Mass Tran. 48 (13) (2005) 2652–2661.

[59] Bogumiła Kumanek, Dawid Janas, Thermal conductivity of carbon nanotube networks: a review, J. Mater. Sci. 54 (10) (2019) 7397–7427.

[60] Min-Sheng Liu, Mark Ching-Cheng Lin, I-Te Huang, Chi-Chuan Wang, Enhancement of thermal conductivity with carbon nanotube for nanofluids, Int. Commun. Heat Mass Tran. 32 (9) (2005) 1202–1210.

[61] R.L. Hamilton, O.K. Crosser, Thermal conductivity of heterogeneous two-component systems, Ind. Eng. Chem. Fund. 1 (3) (1962) 187–191. .

[62] D. Jing, Y. Hu, M. Liu, J. Wei, L. Guo, Preparation of highly dispersed nanofluid and CFD study of its utilization in a concentrating PV/T system, Sol. Energy 112 (2015) 30–40. .

[63] J.A. Duffie, W.A. Beckman, W.M. Worek, Solar Engineering of Thermal Processes, fourth ed., Wiley, 2013 https://doi.org/10.1115/1.2930068.

[64] A.A. Sagade, N.N. Shinde, P.S. Patil, Effect of receiver temperature on performance evaluation of silver coated selective surface compound parabolic reflector with top glass cover, Energy Proc. 48 (2014) 212–222, https://doi.org/10.1016/j.egypro.2014.02.026.

[65] B.O. Bolaji, Flow design and collector performance of a natural circulation solar water heater, J. Eng. Appl. Sci. 1 (1) (2006) 7–13.

[66] Kotturu Mouli, V.V. Chnadra, L. Syam Sundar, A.M. Alklaibi, Zafar Said, K. V. Sharma, V. Punnaiah, Antonio CM. Sousa, Exergy efficiency and entropy analysis of MWCNT/Water nanofluid in a thermosyphon flat plate collector, Sustain. Energy Technol. Assessments 55 (2023), 102911.

[67] Devendra Singh, Ajay Kumar Sharma, Ritvik Dobriyal, Vipul Paliwal, Experimental performance of flat plate solar collector using Al_2O_3-water nanofluid, in: AIP Conference Proceedings, vol. 2521, AIP Publishing, 2023 no. 1.

[68] Zafar Said, Prabhakar Sharma, L. Syam Sundar, Changhe Li, Duy Cuong Tran, Nguyen Dang Khoa Pham, Xuan Phuong Nguyen, Improving the thermal efficiency of a solar flat plate collector using MWCNT-Fe3O4/water hybrid nanofluids and ensemble machine learning, Case Stud. Therm. Eng. 40 (2022), 102448.

[69] M.S.R.M.S. Faizal, Rahman Saidur, Saad Mekhilef, A. Hepbasli, I.M. Mahbubul, Energy, economic, and environmental analysis of a flat-plate solar collector operated with SiO 2 nanofluid, Clean Technol. Environ. Policy 17 (2015) 1457–1473.

[70] Ehsan Farajzadeh, Saeid Movahed, Reza Hosseini, Experimental and numerical investigations on the effect of Al2O3/TiO2H2O nanofluids on thermal efficiency of the flat plate solar collector, Renew. Energy 118 (2018) 122–130.

[71] Seyed Ebrahim Ghasemi, Ali Akbar Ranjbar, Thermal performance analysis of solar parabolic trough collector using nanofluid as working fluid: a CFD modelling study, J. Mol. Liq. 222 (2016) 159–166.

[72] De los Rios, Mariana Soledad Bretado, I. Carlos, Rivera-Solorio, J. Alejandro, García-Cuéllar, Thermal performance of a parabolic trough linear collector using Al2O3/H2O nanofluids, Renew. Energy 122 (2018) 665–673.

[73] Alibakhsh Kasaeian, Samaneh Daviran, Reza Danesh Azarian, Alimorad Rashidi, Performance evaluation and nanofluid using capability study of a solar parabolic trough collector, Energy Convers. Manag. 89 (2015) 368–375.

[74] Arun Kumar Tiwari, Vijay Kumar, Zafar Said, H.K. Paliwal, A review on the application of hybrid nanofluids for parabolic trough collector: recent progress and outlook, J. Clean. Prod. 292 (2021), 126031.

[75] M.M. Heyhat, M. Valizade, Sh Abdolahzade, M. Maerefat, Thermal efficiency enhancement of direct absorption parabolic trough solar collector (DAPTSC) by using nanofluid and metal foam, Energy 192 (2020), 116662.

[76] Praveen Kumar Kanti, K.V. Sharma, H.N. Anil Rao, Masoud Karbasi, Zafar Said, Experimental investigation of synthesized Al2O3 Ionanofluid's energy storage properties: model-prediction using gene expression programming, J. Energy Storage 55 (2022), 105718.

[77] Amir Menbari, Ali Akbar Alemrajabi, Rezaei Amin, Experimental investigation of thermal performance for direct absorption solar parabolic trough collector (DASPTC) based on binary nanofluids, Exp. Therm. Fluid Sci. 80 (2017) 218–227.

[78] Ali Akbar Abbasian Arani, Farhad Monfaredi, Nanofluid turbulent flow in parabolic trough collector: insulator roof, acentric absorber tube and SiC nanoparticles effects, Eng. Anal. Bound. Elem. 156 (2023) 160–174.

[79] G. Alvarez, J. Arce, L. Lira, M. Heras, Thermal performance of an air solar collector with an absorber plate made of recyclable aluminum cans, Sol. Energy 77 (2004) 107–113.

[80] J.Y. Liu, Y.J. Zhang, Has carbon emissions trading system promoted non-fossil energy development in China? Appl. Energy 302 (2021), 117613.

[81] A. Mostafaeipour, A. Bidokhti, M.B. Fakhrzad, A. Sadegheih, Y.A. Zare Mehrjerdi, New model for the use of renewable electricity to reduce carbon dioxide emissions, Energy 238 (2022), 121602.

[82] Adnan Alhathal Alanezi, Bassyouni Mohamed, Shereen MS. Abdel-Hamid, Hassn Safi Ahmed, Mohamed Helmy Abdel-Aziz, Mohamed Shafick Zoromba, Yasser Elhenawy, Theoretical investigation of vapor transport mechanism using tubular membrane distillation module, Membranes 11 (8) (2021) 560.

[83] Z. Liu, Z. Yu, Jerry), T. Yang, S. Li, M. El Mankibi, L. Roccamena, et al., Experimental investigation of a vertical earth-to-air heat exchanger system, Energy Convers. Manag. 183 (2019) 241–251.

[84] M.M. Rafique, H.M.S. Bahaidarah, M.K. Anwar, Enabling private sector investment in off-grid electrification for cleaner production: optimum designing and achievable rate of unit electricity, J. Clean. Prod. 206 (2019) 508–523.